The DC size effect and specular surface reflection in cadmium

1990 J. Phys.: Condens. Matter 2 8137

(http://iopscience.iop.org/0953-8984/2/41/003)

J. Phys.: Condens. Matter **2** (1990) 8137–8159. Printed in the UK

The DC size effect and specular surface reflection in cadmium

Jacobus van der Maas† and R Huguenin
Institut de Physique Experimentale de l'Université de Lausanne, CH-1015 Lausanne, Switzerland

Received 30 March 1990, in final form 1 June 1990

Abstract. We present precision measurements of the electrical resistivity ρ on a cadmium single crystal normal to the c-axis below 9 K. The sample thickness d was reduced by chemical polishing from 1.1 to 0.04 mm. ρ depends systematically on the quality of the surface (etching a polished surface results in an increased residual resistivity ρ_0 and a decreased temperature dependence of ρ). A minimum in the temperature dependent part, $\rho - \rho_0$, is observed when the thickness is close to the size of the mean free path. A T^2-variation of the surface resistivity is observed over a limited temperature range. While these features are in qualitative agreement with the Soffer model for specular scattering, the minimum is deeper and the T^2-range more extended than predicted by this model. The results are compared with existing size effect data on copper and potassium.

1. Introduction

Size effects in the electrical resistivity ρ are of importance when the bulk electron mean free path $l(T)$ is comparable with or larger than the characteristic sample dimension d. This situation is encountered when a bulk property is to be measured on pure samples, as e.g. the measurement of the T^2 electron–electron scattering contribution to the bulk resistivity ρ_∞, or the measurement of the specific resistivity of lattice defects like dislocations.

The temperature dependence of the size effect (size-induced deviations from Matthiessen's rule: SIDMR), can be calculated by solving the Boltzmann equation with a boundary condition imposed on the electron distribution function, a calculation first performed for the film geometry by Fuchs (1938), and for the wire geometry by Dingle (1950). The large number of available experimental results (reviewed for example by Bass 1972, 1982) are not satisfactorily explained by this model. Predicted size-effect corrections, both on the residual resistivity ρ_0 and on the temperature dependent part of the electrical resistivity, $\rho - \rho_0$, are inconsistent with the data. To get insight into the largely unknown SIDMR, Van der Maas *et al* (1981b, c) performed an empirical analysis of existing data, concluding at the general existence of a T^2 contribution induced by surface scattering, which would influence the interpretation of data on electron–electron resistivity.

† Present address: Ecole Polytechnique Fédérale Lausanne, LESO-PB, CH-1015 Lausanne, Switzerland.

0953-8984/90/418137 + 23 $03.50

An explanation for this apparent T^2-dependence was given by Sambles and Preist (1982) who have shown that by taking the boundary conditions of Soffer (1967) instead of Fuchs, most of the SIDMR observed in wires and films may be explained using only two parameters (i) the ratio $\kappa(T) = d/l(\infty, T)$, of the characteristic sample dimension d to the bulk mean free path $l(\infty, T)$, and (ii) the roughness r, ratio of the root mean square height of deviations from the mean surface to the Fermi wavelength.

The resistivity of a sample of thickness d may be written as

$$\rho(d, T) = \rho(\infty, T) + G(\kappa(T), p(r))\, \rho l/d. \tag{1}$$

The enhancement function G is an integral expression determined by the geometry (film or wire), and depends on the parameter κ and on the specularity parameter $p(r)$. The latter is a function of the angle of incidence of the conduction electrons with the surface, parametrised by Soffer's roughness parameter r. SIDMR are given by the temperature dependent part of $\rho(d, T) - \rho(\infty, T)$. In this model the product $\rho l = \rho(\infty, T)$ is a material constant and therefore

$$\kappa(T) = d/l(\infty, T) = \rho(\infty, T)/(\rho l/d). \tag{2}$$

Recently the Soffer–Sambles model was successfully used to fit new experimental data of ρ as a function of thickness (Au films: Stesmans 1983; Ga wires: Boughton 1984; Cu whiskers: Kuckhermann *et al* 1985). Quantitative agreement of the observed SIDMR with the model was reported when r is treated as an adjustable parameter. Indeed a fit of the theory (Kuckhermann *et al* 1985) resulted in an apparent, non-physical decrease of the roughness with increasing thickness. It has become clear that a quasi-T^2 dependence over a limited range in T, is a natural consequence of the Soffer model (Stesmans 1983). Kuckhermann *et al* (1985) showed also that one can correct for the size effect in copper whiskers and deduce the bulk electron–electron scattering resistivity at low temperatures. Similar results have been reported for aluminium (Romero *et al* 1987).

As the theory of the size effect has only been developed for spherical Fermi surfaces in the relaxation time approximation, it is not expected to explain details of data on real metals like tungsten (Sambles and Mundry 1983) or aluminium (Sambles and Elsom 1985). Indeed the following three effects are expected to play a role:

(i) The product ρl will appear to vary with temperature and orientation. This results from the anisotropy of the mean free path, because the (experimental) value of ρl is related to the area of the Fermi surface where $l(T)$ is longest. Indeed, Bate *et al* (1963) show that ρl in equation (1) is multiplied by the ratio $\langle l^2 \rangle / \langle l \rangle^2$ (where the averaging is over the Fermi surface), and the size effect in thick samples ($\kappa > 1$) will be dominated by the longest mean free paths.

(ii) Anisotropy of the Fermi surface will lead to an orientation dependence of the size effect (Risnes and Sollien 1969: Bouillard and Vajda 1979).

(iii) The temperature dependence of the size effect can not be correctly predicted as long as the small-angle scattering nature of low temperature phonons is not taken into account (Risnes 1970, Ehrlich 1971, Kogan and Ustinov 1981).

The relative importance of these effects is not known at the moment. One approach would be to include them all into the Boltzmann equation and proceed to theoretical simulation for a real metal. On the other hand, to stimulate just the development of these detailed theoretical models, new data from well controlled experiments are needed.

We report here experimental results on the effect of surface specularity on the DC size effect in pure cadmium samples below 9 K. Detailed results are obtained on the temperature dependent part of the resistivity when the residual κ-values are of the order of unity. ρ depends systematically on the quality of the surface: etching a polished surface results in an increased residual resistivity ρ_0 and a decreased temperature dependence of ρ. A minimum in the temperature dependent part, $\rho - \rho_0$, is observed when the thickness is close to the mean free path. A T^2-variation of the surface resistivity is observed over a limited temperature range. While these features are in qualitative agreement with the Soffer model for specular scattering, the minimum is deeper and the T^2-range more extended than predicted by this model.

Comparison with the Soffer model is made on a plot of $\rho - \rho_0$ as a function of ρ_0. This way of representing the data on a DMR plot appears to be a sensitive test for smoothness of the data and for comparison between experiment and theory. This test is then applied to the copper data of Kuckhermann *et al* (1985) showing that these data are consistent with Soffer theory without the need of assuming a thickness dependence of the roughness parameter r.

In the following we present the experimental procedure (section 2), the experimental results (section 3) and a discussion including a comparison with existing size effect data on copper and potassium (section 4).

2. The experimental procedure

The starting material for the crystal had 6N grade purity (from Cominco, Canada) and the bulk residual resistance ratio of 2×10^4 (current flow normal to the c-axis) gives a mean free path $l(\infty, 0)$ of $\sim$0.5 mm. For measurements on a full size 13 mm diameter monocrystalline sample with growth axis along $[11\bar{2}0]$ we used a tuning fork geometry (Van der Maas *et al* 1981b), and for the present investigation a piece 2.5 cm in length has been taken from that sample. The configuration of the crystal and its copper support (S) is given schematically in the inset of figure 1. The tuning fork geometry is maintained but an additional side-arm is cut into the crystal and soldered to the support, which has the following functions: (i) strain free support of the sample base (essential to handle thin samples); (ii) thermal contact; (iii) third-current contact to measure the arms of the sample separately. Because the tuning fork slit was parallel to the c-axis, the current flow was always in the basal plane of the hexagonal structure. Cd-Bi low-thermal solder was used and copper-cladded superconducting leads once soldered to the sample, were fixed to the support (S) with Stycast 2850. The contact resistance obtained was less than 1 $\mu\Omega$ below 7 K. Good thermal contact between the support S and a copper thermometer block was obtained by using gallium as solder (Reynolds and Anderson 1976). The sample attached to its support could be, without risk for damage, taken out of the cryostat for room temperature measurement, chemical etching or polishing. The thermometer block was in a vacuum chamber in a ^{4}He cryostat, and its temperature could be varied with a resistance heater.

The initial geometry of the active sample part was that of a 2 mm thick flat plate, 1 cm in length, with an aspect ratio (width/thickness) of about five, which increased to 20 during the thinning procedure (final thickness 0.04 mm). The sample was reduced in thickness by chemical polishing in the solution recommended by Rahn *et al* (1972) which provided an attack rate of about 7 μm min^{-1}, after which the sample was gently rinsed with distilled water and acetone. Etching was obtained by keeping the sample in a 5%

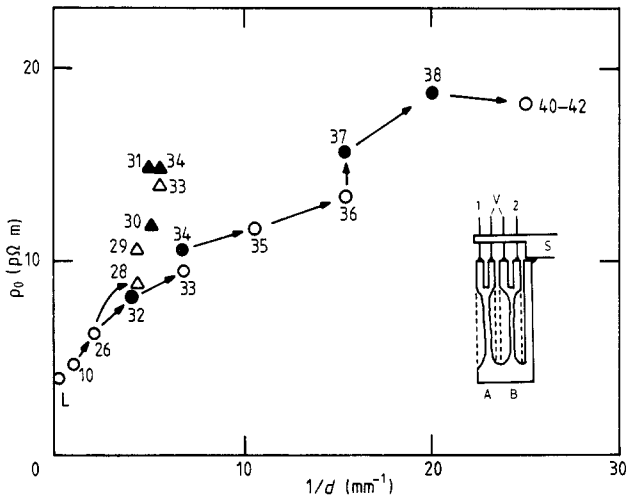

Figure 1. The residual resistivity of flat cadmium samples as a function of inverse thickness. Open symbols: polished; filled symbols: etched; triangles: sample part A; circles: sample part B. L is the full-size sample and arrows indicate the history of the sample (run-numbers are given near each symbol). The changes in going from triangle 28 to 29 and from 30 to 31 result from deliberate bending of the sample. In the inset is shown how the single crystal was cut, and soldered to leads and heat sink: sample parts A and B before (dashed) and after thinning; voltage leads V, heat sink S and three current leads 1, 2 and S.

solution of chloric acid for about 5 min. The sample parts that needed protection against chemical attack, including the support and leads, were covered with an acetone soluble lacquer (Lacomit, Agar Aids, London). Examination with a scanning electron microscope of dummy samples which had received the same polishing treatment as the actual sample showed no structure, the surface being smooth with a resolution limit of 0.2 μm.

Resistance measurements were made with a bridge using a SQUID as null detector and the currents were supplied by a DC current comparator system (Guildline 9975). The ratio of the currents in the arms of the bridge was stable with a precision of 10^{-7}. The sample resistance (10^{-8}–10^{-5} Ω) was measured by comparing with a resistance of 1 $\mu\Omega$, which was kept in the 4 K bath. The latter resistance was made out of stock copper–phosphor alloy, and had a sandwich structure as proposed by Barnard and Caplin (1978). The absence of current dependence was checked and the resolution below 7 K, was typically 3 ppm with a 10 mA current in a 1 $\mu\Omega$ sample and a 1 s time constant. Low resolution measurements (1%) were possible at temperatures where the NbTi leads were not superconducting (9–11 K).

The temperature measurement was made with a calibrated germanium thermometer (Lake Shore GR-200A). Temperature was regulated in a proportional-integral feedback loop controlled by a 16-bit microcomputer system allowing to set and stabilize the thermometer resistance to 0.01%. The temperatures could be reproduced to <1 mK at 9 K, and better below.

For the conversion from resistance R to resistivity ρ the geometrical factor R/ρ was determined to better than 0.1% at room temperature using for the resistance of cadmium (current flow normal to the c-axis): $\rho(t\,^\circ\mathrm{C}) = 6.3\ (1 + 0.0043\,t)$ $\mu\Omega$ cm (Rowlands *et al* 1978). While this procedure to convert low temperature data may be in error by a few per cent, intercomparison of the data at a 0.1% level is justified however, as long as the error is systematic (which is the case here).

The absolute thickness and width of the sample measured with an optical microscope was not better known than about 10% because the initial plate geometry becomes irregular after chemical thinning. Therefore the sample thickness d was estimated from both the dimensions and the changes in the geometrical factor.

3. Experimental results

Experimental surface resistivity data are presented in figures 1 to 5. Figure 1 shows the historic development of the residual resistivity of the cadmium sample resulting from the procedures of chemical polishing (open symbol) and etching (filled symbol) as a function of inverse sample thickness, $1/d$. The numbers next to each symbol refer to the sequence of 42 runs during which the measurements were made.

To avoid the extrapolation uncertainty in ρ_0, which can be important when intercomparing data, the residual resistivity ρ_0 has been replaced in this and following figures

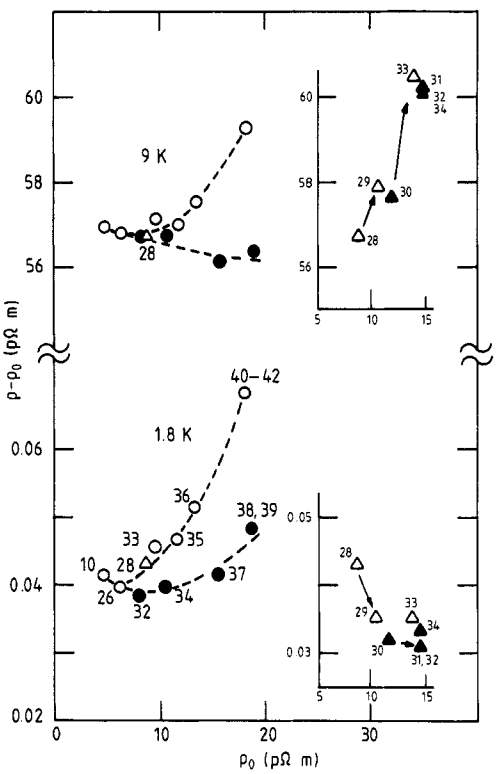

Figure 2. The temperature dependent part of the resistivity $\rho - \rho_0$, as a function of residual resistivity ρ_0, at 1.8 and 9 K. The symbols and numbers are the same as in figure 1. Dashed curves are drawn through the data points to guide the eye and for later reference (figure 10). The changes in going from triangle 28 to 29 and from 30 to 31 (see inset), result from deliberate bending of the sample.

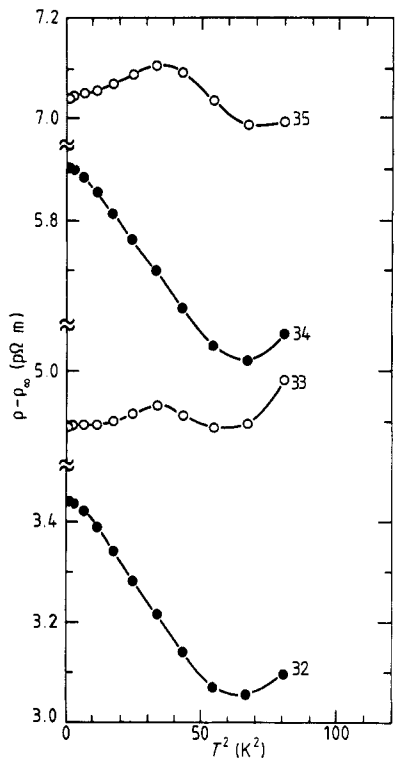

Figure 3. The surface resistivity $\rho - \rho_\infty$ as a function of T^2 for runs 32–35 (sample part B). The etched 250 μm sample (:32), is polished down to 150 μm (:33), changing a strong negative temperature derivative into a positive one, with a maximum around 6 K. Subsequent etching (145 μm: 34) and polishing (95 μm: 35), shows that the change is reproducible while being more pronounced for small thicknesses.

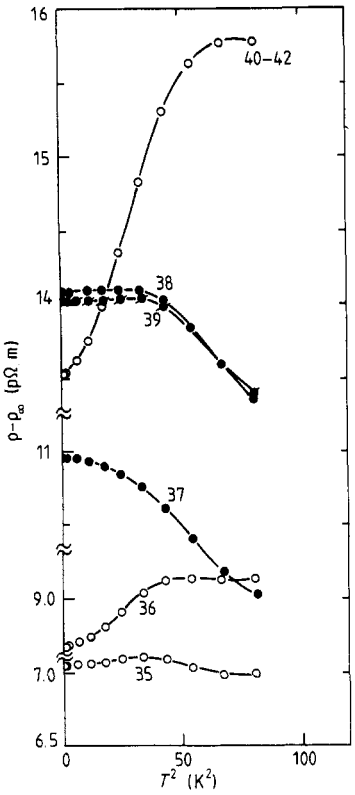

Figure 4. The surface resistivity $\rho - \rho_\infty$ as a function of T^2 for runns 35–40 (sample part B). The polished sample (95 μm: 35) is thinned by polishing (65 μm: 36), etched with HCl as usual (65 μm: 37), etched with HNO_3 (50 μm: 38), recycled to room temperature (:39), polished (40 μm: 40) and twice recycled to room temperature (41, 42).

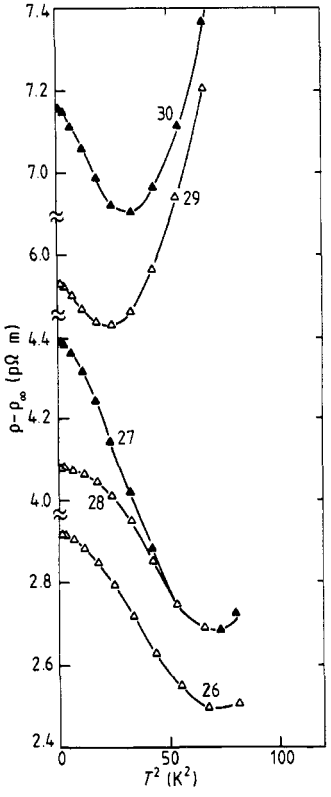

Figure 5. The surface resistivity $\rho - \rho_\infty$ as a function of T^2 for run 26–30 (sample part A). The polished 350 μm thick sample (:26) is etched (250 μm: 27), and repolished (230 μm: 28). After bending the sample (:29) the residual resistivity increased by about 2 pΩ m, while the temperature dependence increased considerably above 6 K. Subsequent etching (:30) resulted in both an increased residual resistivity and a reduced temperature dependence.

by the resistivity at 1.3 K (called ρ_0), being the lowest temperature at which, in all runs, a data point is available.

The lowest ρ-value, ρ(L), (point marked 'L' in figure 1) corresponds to the full-size sample (Van der Maas *et al* 1981a). The measurements made after the mounting of the newly prepared sample were used to test the reproducibility. A decrease in ρ_0 was observed during the first two weeks (run 1–10, table 1) which we attribute to room temperature anneal. At the end of these test-runs the resistivity had stabilized and even annealing in air at 150 °C could not decrease ρ_0 further. Also the residual resistivity of 4.6 pΩm, corrected for surface scattering (table 1, column 3) is very close to ρ(L). We then adopted the sample measured in run 10 (ρ(10), d = 1.1 mm) as a reference. In the following, the temperature dependence of the bulk resistivity, $\rho(T, \infty) = \rho_\infty$, has been identified with that of the reference resistivity, ρ(10). The difference $\rho(10) - \rho_\infty$ is by definition constant at all temperatures. The measured resistivity $\rho(T)$, is fitted to the

Table 1. Characteristic size d, and fit parameters ρ_0, A and B (figure 7); run numbers from figure 1.

	d (mm)	ρ_0 (pΩ m)	$\frac{3}{8}(\rho l/d)$†	A (fΩ m K^{-2})	B (fΩ m K^{-5})
L	6.5	3.88	0.11	15	0.8
Run 1	2	5.32	0.4	20	0.9
Run 10	1.1	4.64	0.75	14.7	0.89
Run 27B	0.5	6.79	1.5	2.5	—
Run 40B	0.04	18.0	19	65	—

† Size effect correction for thick films (Fuchs 1938).

power law $\rho = \rho_0 + AT^2 + BT^5$ (Van der Maas *et al* 1981a) over the temperature interval 1–9 K. From the coefficients given in table 1, it is seen that the temperature dependence is essentially the same for ρ(L) and for ρ(10). From run 26 on, when the average thickness was reduced to 0.5 mm the two arms A and B of the sample (inset figure 1) were studied separately. While sample B (circles figure 1) was alternately polished and etched, down to a thickness of 40 μm (32 → 40), sample A (triangles figure 1) was used to study the effect of deformation in a control experiment (28 → 34). Indeed by bending sample A we increased ρ_0 first by 2 pΩ m (28 → 29) and then by 3 pΩ m (30 → 31). No change in B was observed when sample A was deformed.

We observe in figure 1, both for part A and B, that polished surfaces have systematically a lower residual resistivity, and etching a polished surface always increases ρ_0 (e.g. 29 → 30, 33 → 34, 36 → 37). This result, corresponding to the intuitive idea that increased roughness increases the influence of the surface, is found in all models of surface scattering and is confirmed by extensive experimental data (e.g. Stesmans 1982, Thummes *et al* 1985).

In figure 2, the temperature dependent part, $\rho - \rho_0$, is given as a function of residual resistivity, ρ_0, at 1.8 and 9 K. Symbols and numbers are the same as in figure 1. Curves are drawn through the data points to guide the eye. At 1.8 K, thinning the sample first decreases $\rho - \rho_0$ (10 → 32), while a further decrease in thickness causes $\rho - \rho_0$ to increase with ρ_0, slowly for etched and rapidly for polished surfaces. A minimum results which, for the etched surfaces, is deepest and broadest. It is observed that etching a polished surface always decreases $\rho - \rho_0$. For higher temperatures, the picture is the same but the minima shift to higher ρ_0 (smaller values of d).

The arrows in the insets at 1.8 and 9 K point to the effect of bending on $\rho - \rho_0$ (triangles 28 → 29 and 30 → 31). At 1.8 K $\rho - \rho_0$ is considerably reduced while at 9 K on the contrary a large increase is observed. The effect of etching on the deformed samples is still present but is less pronounced than for undeformed samples of the same thickness (29 → 30 and 33 → 34).

Figures 3, 4 and 5 show the temperature dependence of the surface resistivity, $\rho - \rho_\infty$. For easy identification of T^2-like behaviour $\rho - \rho_\infty$ is plotted as a function of T^2. The curves in figures 3 and 4 correspond to sample part B as measured in runs 32–42. We note that there exists a temperature range over which the surface resistivity varies quadratically with temperature, with a coefficient which can be positive or negative.

In figure 3, the surface resistivity in run 32 (250 μm thick sample with etched surface) strongly changed after polishing the sample to a thickness of 150 μm (:33). Indeed the initial negative temperature coefficient over the whole temperature range becomes positive below 6 K and a maximum appears. To determine whether this is due to the change in thickness or if it is an effect of surface roughness the sample is etched

without noticeable change of size. Surprisingly the etching restores practically the former temperature dependence (compare 34 with 32). By subsequently polishing down to a thickness of 95 μm (:35), the features observed for the high surface polish (:33) appear again but more pronounced.

In figure 4, the result for run 35 is given for comparison with figure 3. Polishing to 65 μm (:36) increases the temperature dependence of the surface resistivity considerably, the maximum has shifted to $\simeq$7 K. Etching without noticeable change in thickness (:37) gives again a lower temperature variation of ρ than the bulk over most of the temperature range. A small maximum (not visible on the plot) appears near 2 K. Continued etching to 50 μm (:38, 39) causes the maximum to broaden and to shift to $\simeq$6 K. The sample repolished shows a more than fourfold increase of the surface resistivity for 40 μm (:40) with respect to 65 μm (:36) and a shift of the maximum to $\simeq$8.5 K. The last run has been repeated for reproducibility (:41, 42).

In figure 5, we switch the attention to sample part A which has been measured simultaneously with part B and served as a control experiment. On the other hand while B remained unchanged, we have studied the effect of deformation on the size effect on part A. In run 26, the surface resistivity of polished sample A (350 μm), shows a very small maximum at $\simeq$2 K. Polishing down to 250 μm and making the surface rough by etching (:27) increases the residual surface resistivity by approximately 50% while decreasing considerably the temperature dependence of ρ. Interestingly, polishing the surface for a short time (:28, 230μ), results in an appreciable decrease in $\rho - \rho_\infty$ at temperatures below 7 K, but it does not affect ρ above 7 K. Although with a broadened maximum, we returned almost to the temperature dependence of the thicker sample (:26). At this point the sample was slightly deformed (:29). As a result, ρ_0 increased by 1.9 pΩ m, the maximum in $\rho - \rho_\infty$ around 2 K (:28) disappeared, and a minimum appeared near 5 K. Indeed the temperature dependence decreased below, but increased very strongly above 5 K (:29). Etching of the deformed sample has still an effect (:30), deepening the minimum (shift to $\simeq$6 K), and decreasing the temperature dependence in general. The second deformation (30 $\rightarrow$ 31 see figure 2, not shown in figure 5) increased ρ_0 further by $\simeq$3 pΩ m, shifted the minimum in $\rho - \rho_\infty$ to lower temperature ($\simeq$4 K), while increasing the overall temperature dependence.

4. Discussion

In an empirical size effect study (Van der Maas *et al* 1981) we noted that the data in the literature show considerable scatter and one of the objectives of this study was to find out what the origin of this scatter could be. To understand why some authors found no SIDMR where others did. We wanted to know for instance whether the data are most sensitive to lattice defects introduced during the sample preparation or whether the condition of the surface is the most important source of scatter in the data. The questions which oriented the present study included:

(i) Is it possible to reproducibly change the quality of the sample surface?
(ii) Is there a systematic influence of the surface condition on SIDMR?
(iii) Can the quality of the surface be used as a test for size effect theories?
(iv) Is the size effect noticeable in relatively thick samples?

Indeed there are no systematic data on $\rho(d, T)$ where the residual value of the parameter $\kappa = d/l$ is larger than unity and where the surface specularity has been changed sys-

tematically by alternate polishing and etching of the samples. Cadmium is a good candidate for such an investigation as the polishing procedure is well under control and the chemical attack can be made very uniformly without making holes in thin samples. The reproducibility of the data also shows that we succeeded in avoiding mechanical damage by careful handling of the samples.

We will now discuss in turn: (i) the thickness dependence of the residual resistivity; (ii) the temperature dependence of the bulk resistivity of cadmium, ρ_∞; (iii) the thickness dependence of the temperature dependence in comparison with the empirical description based on DMR plots; (iv) the measured surface resistivity $\rho - \rho_\infty$ compared with the theoretical models; (v) comparison of the data on cadmium with recent data on Cu and K.

4.1. The thickness dependence of the residual resistivity

We compare the variation of the residual resistivity with thickness as presented in figure 1, with the Fuchs and Soffer theories which assume free electrons and scattering isotropy. The latter assumptions are reasonable for this case, because residual impurity scattering is large angle scattering and therefore isotropic. As shown in figure 6, the theoretical curves (calculated from equation (6) below) indeed reproduce the experimental data very well.

We determine the value of the constant product ρl from the data with etched surfaces because diffuse surface scattering can reasonably be assumed then. In that case the curves from either theory, Fuchs ($p = 0$) or Soffer ($r = \infty$), are superimposed as seen in figure 6. Only one parameter is left in the model and the best fit to the etched sample data in figure 1, yields $\rho l = 2.0 \pm 0.1$ fΩ m^2.

In fitting the data for polished surfaces with the Fuchs model, no single p-value is satisfactory, the thickest samples tending to $p = 0$ while for the thinnest samples $p = 0.2$ (dotted curve in figure 6). On the other hand with the Soffer model, a single value of $r = 0.8$ gives a reasonable fit for all thicknesses, and it has the attraction that the roughness parameter r has a physical meaning, which in principle could be determined in an independent way by microscopic surface analysis (Sambles and Preist 1982). We note however that, with a less extended range in $1/d$ or slightly more scatter in the data, it would have been hard to favour any of these two models.

It remains to be seen whether our assumption of diffuse scattering for the etched surfaces is acceptable because transverse electron focusing experiments by Tsoi *et al* (1979) have shown that specular reflection from surfaces is the rule rather than the

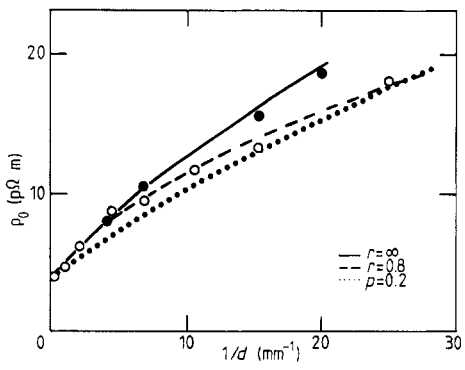

Figure 6. The residual resistivity as a function of inverse thickness (cf figure 1). The etched sample data (full circles) are fitted to the Soffer model with $\rho_\infty(T = 0) = 4$ pΩ m, $r = \infty$ (i.e. $p = 0$), and $\rho l = 2$ fΩ m^2. The broken curve through the polished sample data (open circles) corresponds to the Soffer model with $r = 0.8$, and the dotted curve to the Fuchs model with $p = 0.2$.

exception. Therefore we estimate ρl also in the high-κ limit (using 'thick' samples and high temperature data, as recommended by Sambles and Preist, 1982) where its value is virtually the same over a wide range in roughness r. Indeed at 8 K, where κ is much larger than unity, our data are also consistent with $\rho l = 2.0 \pm 0.1$ fΩ m^2.

This result is in fair agreement with other author's data. For example Bouillard and Vajda (1979) quote 1.83 fΩ m^2 for polycrystalline Cadmium. These authors, studying the anisotropy in the size effect in single-crystal cadmium foils at 4.2 K, found ρl to be about 20% lower in the direction of the c-axis than normal to it. Their [11$\bar{2}$0] samples were polished in an identical way as ours, but assuming diffuse surface scattering they obtained $\rho l = 1.64$ fΩ m^2 in samples with $d < 60$ μm. With the same unrealistic assumption of diffuse scattering (i.e. $p = 0$), we find $\rho l \simeq 1.5$ fΩ m^2 for our polished samples, which is close to their result. This agreement is evidence that the geometry of our samples was not significantly affected by the thinning procedure. Indeed, in Bouillard and Vajda's measurements the initial flat sample was only 70 μm whereas our starting sample was 2 mm thick.

We note finally that these experimental values of ρl for cadmium, are about three times the free electron value of 0.6 fΩ m^2, a discrepancy which has often been observed in size effect measurements (Bass 1982), and which is qualitatively understood from the anisotropy of mean free paths in a real metal (Bate *et al* 1963).

4.2. The temperature dependence of the bulk

The temperature dependence of our 1.1 mm thick reference sample $\rho_\infty = \rho(10)$ is very close to ρ_L, measured on a full size ingot (Van der Maas *et al* 1981a). Moreover the difference in residual resistivity can be carefully estimated from Fuchs' (1938) expression for thick films (table 1). A power law fit, $\rho = \rho_0 + AT^2 + BT^5$, over the whole temperature range of our measurements (1–9 K), yield systematic departures as large as 8% of the experimental values for $\rho - \rho_0$ (figure 7(*a*), (*b*)). Taking a smaller temperature interval (1–4 K) does not significantly improve the fit, leaving the coefficients A and B practically unchanged. This suggests that the power law expression is only a gross approximation. Nevertheless, for reasons of comparison with other data, we maintain this description and for some samples the coefficients are given in table 1. This fit function is taken as the bulk resistivity $\rho(\infty, T)$ in the calculation of $\rho(d, T)$ from equations (1) and (2). We have checked that the systematic errors resulting from the use of this function are not causing the differences found between measured and calculated size effects (see below). We recall that the fit function $\rho(\infty, T)$ does not play a role in the experimentally determined surface resistivity $\rho - \rho_\infty$ (figures 3–5), because experimental values are used for ρ_∞.

While the term BT^5, which is dominating above 3 K, is certainly related to electron–phonon scattering it is questionable whether AT^2, dominating below 2 K, can be identified with an electron–electron scattering term $A_{ee}T^2$. The following estimate can be made from radio frequency size effect experiments (Probst *et al* 1980). A term $\alpha_{ee}T^2$ has been observed in the scattering rates of electrons in Cd with $\alpha_{ee} = 6 \times 10^6$ s^{-1} K^{-2}. To relate A_{ee} and α_{ee} we use the free electron expression (Van der Maas *et al* 1985)

$$A_{ee} = (6\pi^2\hbar/e^2)(1/v_F S_F)\,\alpha \tag{3}$$

where v_F is the Fermi velocity and S_F the area of the Fermi surface. The measured values of α_{ee} yields $A_{ee} = 4$ fΩ m^2 K^{-2}, about a factor four smaller than our experimental value listed in table 1. This suggests that only part of A is due to electron–electron scattering.

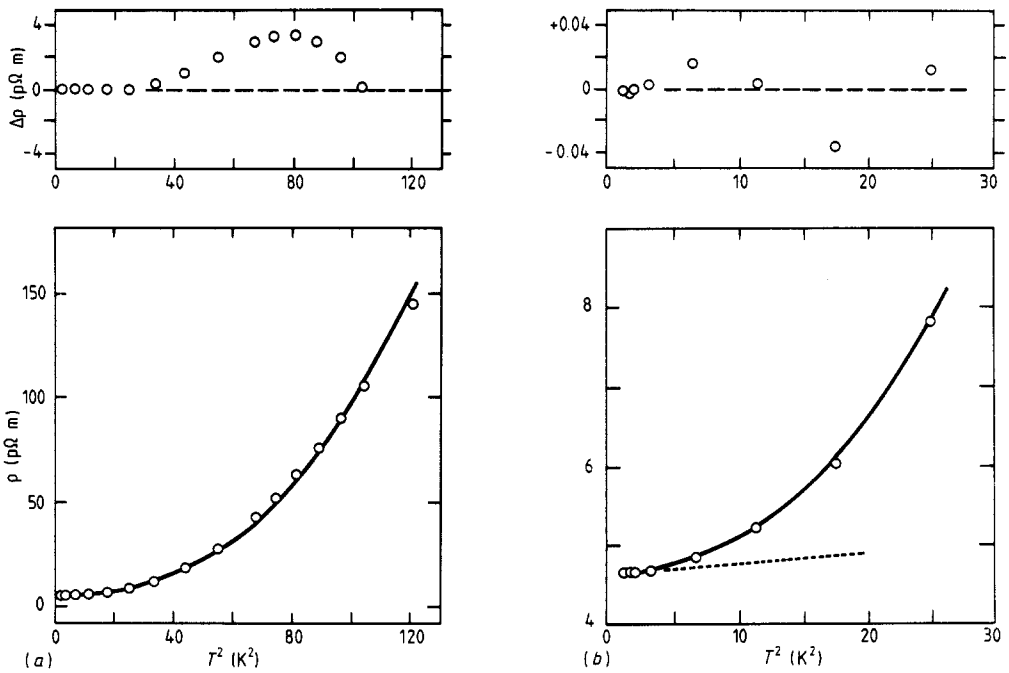

Figure 7. The electrical resistivity of the bulk ρ, as a function of T^2 (*a*) up to 11 K; (*b*) below 5 K. The total resistivity is given in the lower part, where the fitted curve through the data points corresponds to the function $\rho(T) = 4640 + 14.7T^2 + 0.89T^5$ fΩ m. The differences $\Delta\rho$, between this fitting function and the experimental values, are plotted at the top of each figure. Dotted line is the T^2-term.

In a recent paper Lawrence *et al* (1986) have shown that a T^2-term in the scattering rate of some groups of electrons may also be due to phonon scattering because of the particular shape of the Fermi surface of cadmium. This may make the interpretation of the experimental value of A even more complicated.

4.3. Empirical description of the temperature dependence of $\rho(D, T)$

The first observations of the influence of sample size on the temperature dependence part of the resistivity were made by Andrews (1949) and Olsen (1958), who noted that this influence was much more important than the theories of Fuchs (1938) for films, and Dingle (1950) for wires, predicted. These theories model the size effect by solving the Boltzmann equation for a free electron gas and imposing boundary conditions on the electron distribution function. The poor agreement with the experiments showed, however, that this mechanism provided no sufficient explanation.

Feeling the need for new models and new ideas to explain the vast amount of experimental size effect data we performed an empirical analysis of data on a large number of metals (Van der Maas *et al* 1981b, c). This work was inspired by the success of the empirical description of DMR due to impurity scattering (Cimberle *et al* 1974). The latter work has been very helpful, firstly for intercomparison of experimental data and secondly for the testing of models and theories of electron transport in metals (Kaveh and Wiser 1980). Therefore before comparing the data with existing theories in the next section, we will discuss the new data in terms of the empirical description.

The traditional way of analysing DMR data (Bass 1972, Cimberle *et al* 1974) is to plot the temperature dependent part $\rho - \rho_0$ as a function of the residual resistivity ρ_0 generally on a logarithmic scale. In this way, data from different origin can be conveniently compared. For example DMR plots helped in the discussion of the influence on $\rho - \rho_0$ of scattering by impurities (Cimberle *et al* 1974), dislocations (Rowlands and Woods 1975, Fujita and Ohtsuka 1977), vacancies (Nakamura *et al* 1976), and surfaces (Bass 1972). Each source of DMR appears to have its own signature. For the case of varying impurity scattering at a given temperature, $\rho - \rho_0$ increases linearly with the logarithm of ρ_0 and the temperature dependence of this DMR (the slope $d\rho/d \log \rho_0$) can then be analysed (Cimberle *et al* 1974). When ρ_0 is changed by surface scattering, it has been observed that $\rho - \rho_0$ increases linearly with ρ_0 (Neighbor and Newbower 1969; Bass 1972; Van der Maas *et al* 1981b, c). A residual resistivity increase due to dislocations was found to decrease $\rho - \rho_0$ (Rowlands and Woods 1975, Fujita and Ohtsuka 1977). Most of the features of DMR can be traced back to the different anisotropies of the various electron scatterers. The two band model proposed by Dugdale and Basinski (1967) explains the physical mechanism, which has been elaborated in detail by the Bar-Ilan group (Kaveh and Wiser 1980, 1986, Bergmann *et al* 1982, Watts 1985). In this light, dislocations are recognized as the general source of negative DMR because their scattering anisotropy in k-space is similar to that of phonons. The scattering from surfaces is very anisotropic both in real space and in k-space, and we expect DMR (i.e. non-additivity of different scattering mechanisms) to occur. Strictly speaking, as long as the 'normal' size effect (i.e. from space anisotropy of the distribution function) is not known, DMR from surfaces can not be separated out (Bass 1972, 1982). In an empirical approach however 'normal' and 'beyond the normal' (Bass 1972) are lumped together.

A number of features in existing size effect data (Van der Maas *et al* 1981b, c, 1983) like the linearity of DMR plots, the T^2-dependence of the DMR and the decrease of the residual resistivity with increasing specularity, need closer insection or verification.

4.3.1. Size effects. In figure 2, $\rho - \rho_0$ is plotted as a function of ρ_0 at 1.8 and 9 K (at intermediate temperatures the behaviour is similar), and a quasi-linear dependence is only observed for relatively thin samples and low temperatures. A minimum appears in $\rho - \rho_0$ at approximately $d = l(\infty, T)$ and extrapolation to infinite samples size beyond the minimum ($\kappa \geqslant 1$) is complicated, and certainly not linear as we have suggested earlier (Van der Maas *et al* 1983).

Our data gives details on $\rho - \rho_0$ for $\kappa(T = 0) > 1$. Indeed this is the range where $\rho - \rho_0 \ll \rho_0$ and a high measurement resolution with a good reproducibility in sample preparation are required. The data show a clear correlation of $\rho - \rho_0$ with surface treatment, similar to what is observed in noble metals (Stesmans 1982; Van der Maas *et al* 1983). The general rule is that etching a polished sample always reduces the temperature dependent part $\rho - \rho_0$ while increasing the residual resitivity ρ_0.

In figures 3 and 4 typical data for the surface resisitivity $\rho - \rho_\infty$ are plotted as a function of T^2. The temperature dependence is close to quadratic over a considerable range in T, and for the thicker samples with an etched surface the T^2-coefficient is negative. It will be clear from these pictures that when fitting the temperature dependence of a sample to a power law expression without knowledge about the surface term, the result will depend on the temperature interval for the fit, and for $\kappa > 1$ a T^2-term noticeably lower than in the absence of surface scattering would be measured (see table 1).

4.3.2. Deformation experiment. To be sure that we measured a size effect and not the

result of a systematic increase of defects due to sample handling, we have studied what happens when we introduce defects in the sample. Therefore we deformed one arm of the sample by bending (part A, inset figure 2), keeping the other arm unchanged. This experiment allowed us to search for evidence for the interaction between the size-effect and defect scattering. Indeed we expect interaction because an added defect resistivity modifies both the bulk temperature dependence (DMR), and (through a reduced mean free path) it changes (non-linearly) the surface resistivity.

We hoped to create mostly mobile dislocations, which in cadmium would anneal out at room temperature in a few days, much like we have observed during runs 1–10 (table 1). However the bending resulted in a permanent resistivity increase. Indeed, microscopic examination of the crystal revealed that the deformation had produced twinning of the crystals (visible under the microscope as parallel lines, ~1 mm distant and at about 45° with the *c*-axis).

The effect of deformation on the surface resistivity is shown in figures 1, 2 and 5. From the strongly increased residual resistivities in figure 1 (triangles), we see that for the same initial bulk resistivity, the formation of crystal defects during the preparation of the samples would lead to large experimental values for ρl. On the other hand the damaged samples continue to be sensitive to the surface polish. Thus with this kind of plot a particular data series can be tested to see whether the sample preparation is well controlled. Scatter can result from both a bad control of the surface quality or of the defect structure. A plot like in figure 1 can reveal whether the quoted bulk resistivity is consistent with the resitivity of the other samples of the series. In this particular case, the residual bulk resistivity has increased by about 50% after the first deformation (:29) and is more than doubled after the second deformation (:31).

The effect of the deformation on the temperature dependence of ρ (figure 2, inset) is at 1.8 K, a decrease and at 9 K an increase. At 1.8 K, the decrease in $\rho - \rho_0$ after the first deformation (28 → 29) is considerable while a second (stronger) deformation does hardly modify $\rho - \rho_0$ further. This behaviour is in qualitative agreement with observations in the DMR after deformation by Rowlands *et al* (1975, 1978) and Fujita and Ohtsuka (1977). The increase in $\rho - \rho_0$ at higher temperatures on the other hand, is stronger after the second deformation (figure 2). We interpret this change as due to an increased bulk temperature dependence (positive DMR). The striking upturn in figure 5 (28 → 29), is then due to the fact that the subtracted bulk resistivity is too small, rather than due to a change in the influence of the surface. From the systematic studies of deviations from Matthiessen's rule (Cimberle *et al* 1974) the dependence of the bulk phonon scattering on the residual resitivity is known for a number of metals, and $\rho - \rho_0$ can typically double for an order of magnitude increase in ρ_0. From figure 2 we see that at 9 K, the value of $\rho - \rho_0$ increased by 5% in going from run to 28 to 33, i.e. for an increase in the bulk residual resistivity of 4.8 pΩ m (figure 1). An increase in the temperature dependence of 5% for a doubling in residual resitivity is then comparable to the DMR in other metals.

Damaging the sample intentionally caused large upturns above 5 K (figure 5,: 29, 30), but in all the plots of $\rho - \rho_\infty$ (figures 3, 4 and 5) small 'upturns' appear systematically near 9 K. This suggests that the subtracted resistivity ρ_∞ (9 K) is about 0.1 pΩ m (0.2%) too small, which could be caused by a few per cent increase in ρ_∞ (0 K) due to sample handling.

Finally, it will be difficult to imagine an experiment which shows the influence of dislocation density on $\rho - \rho_0$ in the presence of a size effect. Deformation experiments in thin pure samples ($\kappa \sim 1$) have to be re-examined.

4.4. Comparison with existing theories

For many years experimentalists have analysed their data with Fuchs or Dingle's theory as the only quantitatively manageable models for size effects. Alternative models (Blatt and Satz 1960, Azbel 1962) used mean free path arguments and the small-angle scattering nature of low temperature electron-phonon scattering. Blatt and Satz (1960) for example, were able to account for the magnitude of the size effect but at the expense of an additional parameter, the ratio of Umklapp to normal scattering. On the other hand they failed to reproduce the expected T^3-behaviour of $\rho - \rho_\infty$ when the thickness d tends to zero. Their model demonstrates interference effects between phonon scattering and the surface in an elegant way.

In the Fuchs–Dingle theory there were a number of points which could not be explained satisfactorily. Among those one can mention the non-constancy of the material constant ρl with temperature, or the fact that the values of ρl were systematically larger, by a factor 2 to 3, than the free electron value:

$$\rho l = (12\pi^3\hbar/e^2)\, 1/S_F. \tag{4}$$

The experiments by various authors on the same metal also produce a large scatter in ρl (Bass 1972, 1982). These disagreements between theory and experiment were attributed to various sources like mean free path anisotropy or bad knowledge of Fuchs specularity parameter p, but no definite conclusion could be achieved as to the main reasons for the discrepancies.

Sambles and collaborators (1980–1985) have shown that many inconsistencies disappear by using the Soffer (1967) model to interpret the experimental data. Soffer used the same form of the Boltzmann equation as Fuchs, but proposed a more realistic model

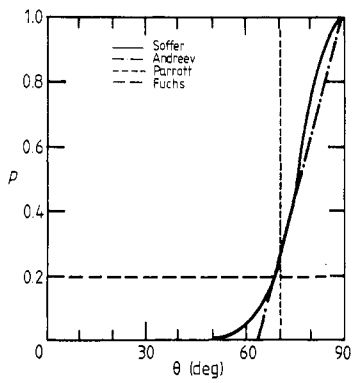

Figure 8. The probability for specular scattering p as a function of the angle of incidence with the normal to the surface, θ, for four surface specularity models: Soffer (full curve, $r = 0.3$), Andreev (chain curve, factor $a = 0.04\ \text{deg}^{-1}$), Parrott (vertical broken line, cut-off angle 70°), Fuchs (horizontal broken line, $p = 0.2$).

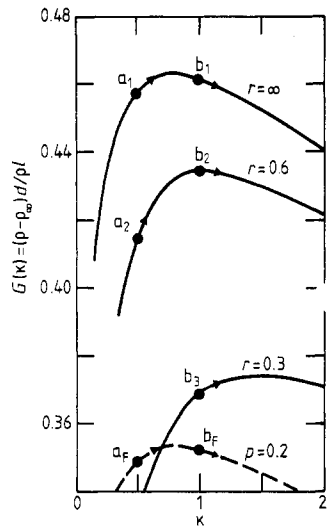

Figure 9. The enhancement factor G predicted by the models of Soffer and Fuchs as a function of κ for diffuse (upper curve, $r = \infty, p = 0$), and specular ($r = 0.6$, $r = 0.3$ and $p = 0.2$) surface scattering.

for the boundary condition at the surface. This model is based on an extension of the discussion of size effects in Ziman's book on *Electrons and Phonons* (Ziman 1960). It takes the geometrical roughness of the surface into account to determine a specularity parameter in the case of electrons hitting the surface under normal incidence. Soffer's extension of the model includes oblique incidence, and more importantly, satisfies the requirement of conservation of the flux of electrons arriving at, and leaving the surface. The result is that in the absence of lateral correlations between the electron wave functions, the specularity parameter of Fuchs theory becomes angle dependent and may be expressed as

$$p_s(\theta) = \exp[-(4\pi r)^2 \cos^2\theta] \tag{5}$$

where θ is the angle of incidence (relative to the surface normal), and $r = h/\lambda$ characterises the surface roughness (h = root mean square height deviations of the surface asperities, λ = electron wavelength).

However there exists other forms for the angle dependent boundary condition $p(\theta)$, and we compare then in figure 8, where models of Soffer (1967), Parrot (1965), Andreev (1971) and Fuchs (1938) are plotted for a particular case of surface specularity. The threee models of Soffer, Parrot and Andreev have the angle dependence in common, and from the example in figure 8 it is seem that a roughness parameter $r = 0.3$ for Soffer (equation 5), is nearly equivalent with a cut-off angle $\theta_0 = 70°$ for the model of Parrot (if $\theta < \theta_0$ then $p = 0$; if $\theta > \theta_0$ then $p = 1$) or with a proportionality factor $a = 0.04\ \text{deg}^{-1}$ for the model of Andreev (if $\theta < \theta_0$ then $p = 0$; if $\theta_0 < \theta < 90°$ then $p = (1 - a(90° - \theta))$).

In order to calculate the size dependent resistivity, a particular model for $p(\theta)$ has to be introduced into the Fuchs formulation and the resulting expression solved by numerical integration. For the present case of thin plates the size dependent resistivity $\rho(d, T)$ is calculated from

$$\frac{\rho(\infty, T)}{\rho(d, T)} = 1 - \frac{3}{2\kappa}\int_0^1 \mathrm{d}u\,(u - u^3)\frac{(1 - p_s(u))(1 - \exp(-\kappa/u))}{1 - p_s \qquad (u)\exp(-\kappa/u)} \qquad (u = \cos\theta). \tag{6}$$

Equivalently the surface resistivity may be expressed as

$$\rho - \rho_\infty = \rho(d, T) - \rho(\infty, T) = G(\kappa, r)\,\rho l/d \tag{7}$$

where G depends on the integral in (6).

If p is constant, equation (1) becomes the Fuchs expression:

$$G = G^{\mathrm{F}}(\kappa, p) \qquad (\mathrm{F\ for\ Fuchs}). \tag{8}$$

It is instructive to plot $G(\kappa, p)$ as a function of κ in order to compare the various models for $p(\theta)$. It is then immediately seen that the predictions for the models of Soffer (1967), Parrot (1965) and Andreev (1971) are very similar but all very different from Fuchs (1938). Therefore we have given in figure 9 some curves of G for Soffer and Fuchs as a function of κ; note that κ increases with temperature. The upper curve is for diffuse scattering where the functions are identical $G(\kappa, r = \infty) = G^{\mathrm{F}}(\kappa, p = 0)$. These functions have the common feature to show a maximum around $\kappa = 1$. But there is an important difference between $G(\kappa, r)$ and $G^{\mathrm{F}}(\kappa, p)$. In the former the maximum is shifted to larger values of κ when the specularity is increased, whereas in the latter the maximum remains at the same κ-value for all values of p. Soffer theory predicts that the temperature dependence of the surface resistivity, i.e. the slope $\mathrm{d}G/\mathrm{d}\kappa$ will increase

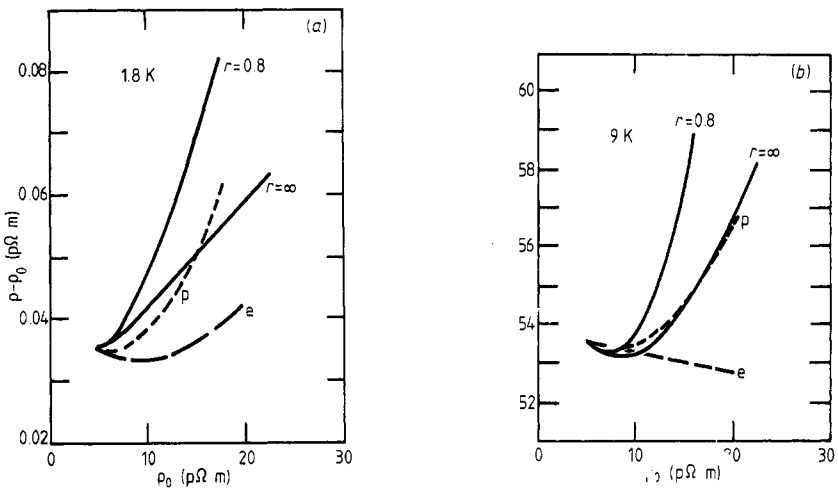

Figure 10. The temperature dependent part of the resistivity $\rho - \rho_0$, as a function of residual resistivity ρ_0, at 1.8 K (*a*) and 9 K (*b*). The broken curves correspond to the experimental results and are the same as in figure 2: etched (e, long-dash) and polished samples (p, short-dash). Theoretical (full) curves correspond to the theory for films with $\rho_\infty(T = 0) = 4$ pΩ m, $\rho\lambda = 2$ fΩ m^2 and two values for the roughness parameter $r = \infty$ and $r = 0.8$ (compare figure 6).

($a_1 \rightarrow a_2$) or will change sign ($b_1 \rightarrow b_2 \rightarrow b_3$ in figure 9) after polishing a sample with $\kappa \simeq 1$, while Fuchs does not ($a_1 \rightarrow a_F$ and $b_1 \rightarrow b_F$). Qualitatively the prediction of the Soffer model agrees with the surprising behaviour shown in figure 3 and 4 where, by polishing the sample surface, the slope of the measured surface resistivity versus T^2 increases, in some cases even changing from negative to positive. We recall however that a shift of the maximum of the enhancement function G is a characteristic of all models where p is a function of the angle of incidence of the electrons on the surface.

In figure 10, we compare the measured temperature dependent part of the resistivity $\rho - \rho_0$ (broken curves, Figures 2 and 10), with the predictions of the Soffer–Fuchs model (full curves, equation 6). In the calculation we have corrected for the fact that $\rho_0 = \rho$ ($d = 1.1$ mm, $T = 1.3$ K). The theoretical curves have been shifted by a fraction of a per cent to have them coincide with the data point for the thickest sample. While the effect of polishing ($r = \infty \rightarrow r = 0.8$) is correctly predicted by an increasing temperature dependence, quite large quantitative differences between theory and experiment are found: the calculated $\rho - \rho_0$ shows a minimum which is narrower, and its increase with ρ_0 is steeper than experimentally observed. Nevertheless Soffer's model reproduces qualitatively the general features of the experimental curves, which remained unexplained by Fuchs model.

We note that any point of a theoretical (continuous) curve in figure 10 corresponds to a certain value of κ. Therefore the geometrical form of the curves depends only on the function G. Changing the values for ρl or the bulk resistivity change both $\rho - \rho_0$ and ρ_0, and the calculated point shifts on the theoretical curve, the latter depending only on the details of the sample geometry and the model for specular scattering. This type of plot is therefore a good test when ρl or the bulk resistivity are uncertain, and will be used in the next paragraph to discuss recent data on copper.

Now that we have seen from the discussion of figures 2 and 10, that the differences

between data and theory can not be removed by a different choice of ρl or $\rho_\infty(T)$ we continue discussing the temperature dependent part of the surface resistivity $(\rho - \rho_\infty)_T$ in figure 11.

In figure 11(a) we consider diffuse surface scattering ($r = \infty$). The thickness is the only free parameter in the model and the steepest decrease in $\rho - \rho_\infty$ is obtained for $d = 500\ \mu$m. It is impossible to reproduce the curve for the 450 μm sample. For thinner samples the model predicts a strong maximum. Curves which come closest in form are the 50 μm sample data and the 240 μm calculated curve. In order to make the model reproduce the steep decrease at low temperatures, κ, i.e. the inverse mean free path, should increase (about ten times) stronger with temperature than through the bulk resistivity alone (equation (2)). However this additional mechanism which would be needed to save this model, should then only be effective as long as $\kappa > 1$, else it becomes incompatible with the thinner sample data where $\kappa < 1$.

The calculated curves for specular surface scattering (figure 11(b)) grow with decreasing r, but because $\rho - \rho_\infty$ calculated for $r = 0.8$ (used for the fit in figure 6) does not produce sufficiently large changes, we show results calculated for the value $r = 0.3$. The polished sample data for $\kappa > 1$, fall well below any curve the theory can generate,

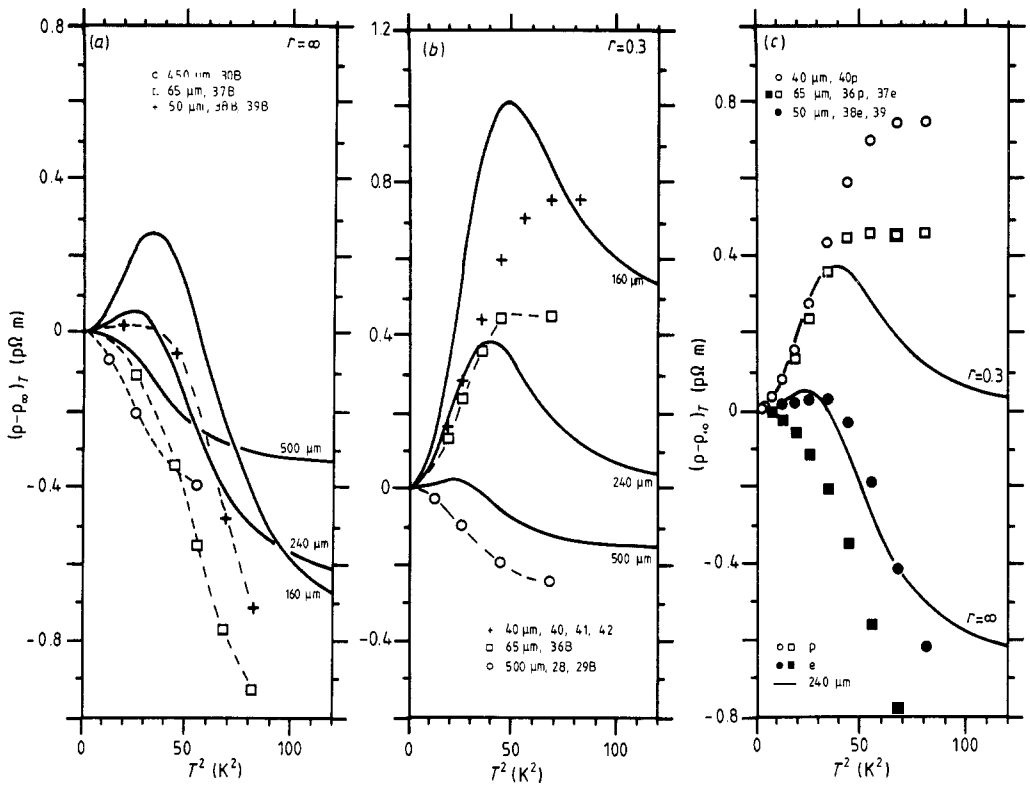

Figure 11. Comparison of the measured temperature dependent part of the surface resistivity $(\rho - \rho_\infty)_T$ with the Soffer model (continuous curves). Broken lines are drawn through the data points to guide the eye (cf figures 3 and 4). Soffer parameters: ρ_∞ as in figure 7, $\rho l = 2$ fΩ m^2. (a) Etched samples, $r = \infty$; (b) polished samples, $r = 0.3$; (c) the effect of polishing; Soffer $d = 240\ \mu$m, $r = \infty$ and $r = 0.3$.

but again curves which come closest in form are sample data near 50 μm and the 240 μm calculated curve.

The data in figures 11(*a*) and (*b*) are replotted in figure 11(*c*), to compare clearly the observed changed in $\rho - \rho_\infty$ after polishing with the model. As was already seen from the plots in figure 10, the model underestimates completely the decrease in surface resistivity for $\kappa > 1$, and underestimates the changes produced by surface specularity.

We do not know the origin for the observed differences, but as we will discuss below with the potassium data, mean free path anisotropy and small angle scattering are likely mechanisms.

4.5. Comparison with results on Cu and K

We have seen that Soffer theory cannot describe quantitatively the size effect in our Cd samples but that it explains qualitatively the strong difference in the temperature dependent resistivity between etched and polished samples. The Cd data suggest that the model underestimates in particular the size effect in real metal samples where κ is about unity, although data in aluminium (Sambles and Elsom 1985) and tungsten (Van der Maas *et al* 1985) could be quite satisfactorily explained. We will now discuss some recent size effect data on Cu and K which show interesting similarities but also differences with the results in Cd.

4.5.1. Copper. Stesmans (1983) analysing his experimental data on gold films with Soffer-Sambles theory found satisfactory agreement and recently Kuckermann *et al* (1985) used the model to interpret their resistivity measurements on Cu whiskers. They obtained a good fit for the thickness dependence of the surface resistivity with $\rho l = 0.66\ \text{f}\Omega\ \text{m}^2$, the free electron value. To fit the temperature dependence of the surface resistivity they had to let the roughness parameter r vary freely; it then appeared to decrease with increasing sample thickness. This kind of observation was also made by Boughton (1984) for Ga. However there is no physical justification for a surface which seems to be more specular in thicker samples, and we found that it could just be an artefact of the fitting procedure.

In Kuckermann *et al*'s analysis the experimental SIDMR were derived using the measured temperature dependence of a 142 μm sample as the bulk resistivity instead of the fit parameters. With this and the value of $\rho l = 0.66\ \text{f}\Omega\ \text{m}^2$ as input parameters they found that the theory of Soffer–Sambles provides a reasonable fit to the data from 12 to 30 K, if the roughness parameter for their etched samples is allowed to vary from $r = 1.7$ for $d = 7\ \mu m$, to $r = 0.32$ for $d = 82.6\ \mu$m. We reproduce their results in figure 12(*a*) at a fixed temperature (20 K) plotting the temperature dependent part of the resistivity $\rho - \rho_0$ as a function of ρ_0. We recall that this type of plot is a severe test of the data as well as of the theory, independent of ρl and ρ_∞. The 142 μm sample is just in the minimum of the family of curves, and includes negative SIDMR. In fact the calculated negative SIDMR of a 142 μm sample increases over the temperature interval 18–34 K from 0.5 to 1.5 pΩ m, which is not a negligible amount. In figure 12(*b*) the same plot is given, but with the curves shifted up by 1 pΩ m. All data points now fall in-between the curves $r = 1.7$ and $r = \infty$ for all temperatures between 18 and 34 K, a much more satisfactory situation for samples with etched surfaces. Fitting the data has now been shifted to the problem how to get access to the bulk which is representative for the samples. The agreement to the data is quite good with practically the same degree of roughness, $r \simeq 2$, for all samples.

The cadmium data of figures 2 and 10 could easily have led to the same kind of conclusion. Indeed without the measurements on the thickest samples, we would have passed the theoretical curves through the data points, shifting them down. The resulting picture of the broken (data) lines crossing the theoretical curves, would exactly correspond to fitting each data point to its Soffer curve as in figure 12(*a*). We conclude therefore that a thickness dependent roughness parameter is likely to be the result of an ill-defined bulk resistivity.

4.5.2. Potassium. In a high resolution study on thin potassium samples an influence of sample size on the temperature dependence was seen, and for the first time it was observed that the temperature derivative of resistivity in thin samples can become negative (Yu *et al* 1984, Zhao *et al* 1988), and the Gurzhi effect is invoked by the authors

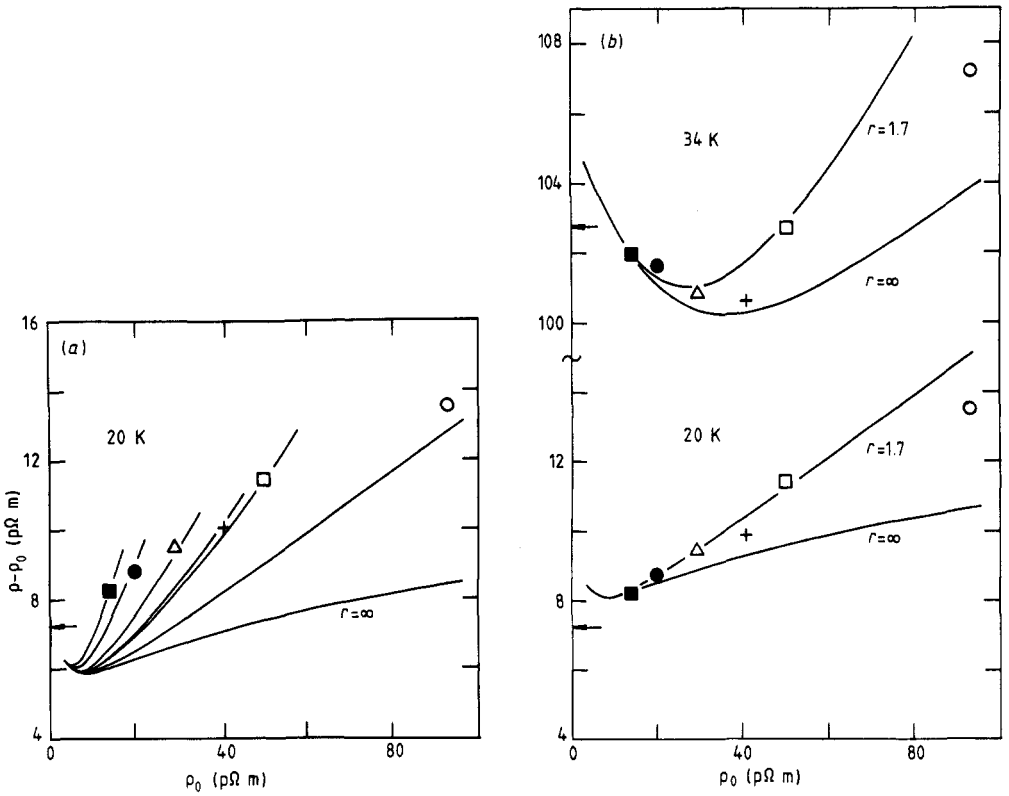

Figure 12. Comparison of the measured and calculated temperature dependent part of the electrical resistivity of copper single crystal wires for different thicknesses and roughness parameter r, as a function of residual resistivity at 20 and 34 K. (*a*) Reconstruction of data from Kuckhermann *et al* (1985) (their figure 2 and table 2). To every data point fits a Soffer–Dingle curve with the roughness r as free parameter and $\rho_\infty(T = 0) = 2.7$ pΩ m, $\rho l = 0.66$ fΩ m^2. (*b*) The calculated Soffer–Dingle curves have been shifted up ≈ 1 pΩ m to fit the data with a single roughness $r = 1.7$. Symbols: (full square) $d = 59$ μm, $r = 0.36$; (full circle) $d = 40$ μm, $r = 0.49$; (triangle) $d = 27$ μm, $r = 0.75$; (cross) $d = 21$ μm, $r = 0.96$; (open square) $d = 14.5$ μm, $r = 1.03$; (open circle) $d = 7.5$ μm, $r = 1.69$. Arrows on the vertical scale give ρ_∞ at 20 and 34 K calculated from their table 2.

(Yu *et al* 1984). It is interesting to compare the negative SIDMR observed in K and Cd, because the relative importance of Gurhi and Soffer effects in these metals are not clear.

In the Soffer model (equations (1), (2) and (6)), a decrease in surface resistivity with increasing temperature results when the mean free path is less than the sample thickness, because an increasing fraction of the sample volume does not experience the presence of the surface. The only T-dependent variable in the model is the bulk resistivity (to calculate a mean free path and κ), and no distinction is made either between small and large angle electron–phonon scattering or normal (NEES) and Umklapp electron–electron scattering (UEES). Therefore two contributions are competing,, the bulk resistivity which is increasing and the surface resistivity which is decreasing with temperature. In the free electron formulation of the Soffer model the bulk resistivity always wins. But we can change the relative contribution of the surface resistivity by adding a mechanism influencing the way electrons reach the surface, without modifying the bulk resistivity. The Gurzhi effect is one of these, NEES does not contribute to the bulk electrical resistivity but it decreases the probability for an electron to reach the surface. Also, small-angle electron scattering (with phonons or dislocations) contributes little to the bulk resistivity, but can modify considerably the way electrons reach the surface.

With this mechanism added, the relative importance of surface resistivity can be quite different in K and Cd. Indeed, the bulk resistivity of potassium at low temperatures contains contributions from electron–phonon scattering (decaying exponentially due to phonon drag) and from Umklapp electron–electron scattering (varying as T^2 and dominating below 1 K), while for cadmium, phonon scattering is still important down to 1 K and both normal and Umklapp scattering contribute to the resistivity.

We note at this point that a negative temperature derivative of resistivity is not basically conflicting with the Soffer model (because it only depends on the relative contribution of surface scattering), and also that the Gurzhi mean free path effect should be included into the Soffer model for a proper treatment.

To see whether the size effect experiments on Cd and K are further comparable, we have analysed the potassium data of Yu *et al* (wire geometry, diameter $0.09 < d < 1.5$ mm), using the Soffer–Dingle model. In order to estimate the roughness parameter we have plotted the data like in figure 1 (not shown). The residual resistivity data then show considerable scatter, similar to what we see in figure 1 when no distinction is made between sample part A and B, and it is not possible to make a fit. At best we can say that the data are consistent with a lowest value for the residual bulk resistivity of 7 pΩ m, $r > 1$ and $\rho l = 3$ fΩ m^2. We attribute the scatter to differences in bulk resistivity due to the polycrystalline nature of the extruded samples, rather than to differences in the surface condition. The experiment shows systematically a decreased temperature dependence for thinner K samples, but the Soffer–Dingle model gives only the right magnitude when going from 1.5 mm to 0.9 mm diameter. For thinner samples, the difference between experiment and theory is qualitatively the same as for cadmium (the theory underestimates completely the experimental result, figures 10, 11), but the effect in potassium is so strong that the temperature derivative of resistivity becomes negative.

A further complication arises when the potassium data are affected by the strain in the polycrystalline samples, the mechanical properties of potassium being very anisotropic. Indeed, in figure 13 we show the effect of deformation on the resistivity of cadmium below 2 K. While the undeformed sample varies similarly to what is expected from the Soffer–Fuchs model (dashed curves), deformation decreases the temperature dependence considerably, both for polished and etched surface condition. Finally, the effects

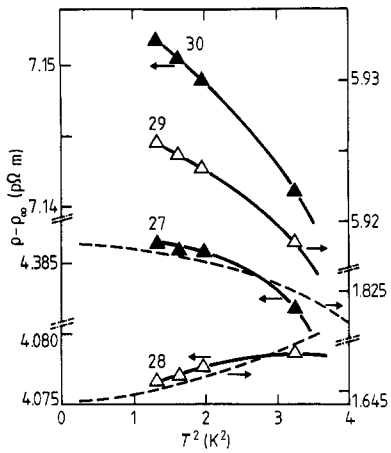

Figure 13. The effect of deformation on the temperature dependence of the surface resistivity below 2 K (sample part A, compare triangles in figures 1 and 2). Before bending, the sample is measured with etched (:27, 250 μm) and polished surface (:28, 230 μm). Subsequent deformation (:29) results in both an increase in residual resistivity (+2 pΩ m) and a decrease in the temperature dependence of ρ. Etching (:30, 200 μm) increases ρ_0 by an additional 1 pΩ m, while making the SIDMR more negative. The broken curves correspond to the Soffer model for $r = \infty$ and $r = 0.3$ ($\rho_\infty(T = 0) = 4$ pΩ m, $\rho l = 2$ fΩ m^2).

observed in K and Cd showing striking similarities, a correct interpretation of K data should be based firstly on a proper size-effect experiment where effects due to strain and surface scattering can be separated, and secondly on using a theory where the Gurzhi effect is incorporated in a Soffer-like model.

5. Conclusion

It has been shown that it is possible to change reproducibly the surface conditions and the size of Cd samples. The changes in the electrical resistivity $\rho(d, T)$ are qualitatively described by the surface scattering Soffer–Sambles models. To account for the drastic changes in the surface resistivity when etching a polished surface, it is essential for the specularity parameter to be angle dependent. The model has also been applied successfully in other metals, like Al, W or Cu. We have shown that some discrepancies between theory and experiment observed in Cu may be related to an ill-defined bulk resistivity. In general the model underestimates negative SIDMR in Cd and the observed T^2-dependence of the surface resistivity is more important and extends over a larger temperature interval than predicted. One should recall that the Soffer model does not take into account small-angle scattering, mean free path anisotropy or Fermi-surface anisotropy. Therefore differences between experimental data and the calculated curves are likely to be due to these simplifying assumptions.

Acknowledgments

We are grateful to Professor Carlo Rizzuto for discussions, to G Burri for SEM surface analysis of the samples and to the Swiss National Foundation for Scientific Research for financial support.

References

Andreev A F 1971 *Sov. Phys.–Usp.* **14** 609–15
Andrew E R 1946 *Proc. Phys. Soc.* **62** 77–88

Barnard B R and Caplin A D 1978 *J. Phys. E: Sci. Instrum.* **11** 1117–22
Bass J 1972 *Adv. Phys.* **21** 431–604
—— 1982 *Landolt–Börnstein New Series* Group III, vol 15 (Berlin: Springer)
Bate R T, Martin B and Hille P F 1963 *Phys. Rev.* **131** 1482–8
Bergmann A, Kaveh M and Wiser N 1974 *Phys. Rev. Lett.* **32** 606–9
—— 1982 *J. Phys. F: Met. Phys.* **12** 2985–3030
Blatt F J and Satz H G 1960 *Helv. Phys. Acta* **33** 1007–20
Boughton R I 1984 *Phys. Rev.* B **29** 4205–10
Boughton R I and Neighbor J E 1972 *J. Low Temp. Phys.* **7** 241–71
Bouillard J-C and Vajda P 1979 *Solid State Commun.* **29** 107–10
Chambers R G 1969 *The Physics of Metals—I: Electrons* ed J M Ziman (Cambridge: Cambridge University Press) 175–89
Cimberle M R, Bobel G and Rizzuto C 1974 *Adv. Phys.* **23** 639–71
Cotti P 1964 *Phys. Kondens. Mater.* **3** 40–74
Dingle R B 1950 *Proc. R. Soc.* A **201** 545–53
Dugdale J S and Basinski Z S 1967 *Phys. Rev.* **157** 552–60
Ehrlich A C 1971 *J. Appl. Phys.* **42** 2598–603
Falkovsky L A 1983 *Adv. Phys.* **32** 753–89
Fuchs K 1938 *Proc. Camb. Phil. Soc.* **34** 100–8
Fujita T and Ohtsuka T 1977 *J. Low Temp. Phys.* **29** 333–49
Greene R F 1966 *Phys. Rev.* **141** 687–92
Haerle M L, Pratt WP Jr and Schroeder P A 1986 *J. Low Temp. Phys.* **62** 397–431
Kaveh M and Wiser N 1980 *Phys. Rev.* B **21** 2278–90
—— 1981 *J. Phys. F: Met. Phys.* **11** 419–28
—— 1986 *J. Phys. F: Met. Phys.* **16** 795–802
Kogan E M and Ustinov V V 1981 *Fiz. Nizk. Temp.* **7** 327–35 (Engl. Transl. 1981 *Sov. J. Low Temp. Phys.* **7** 160–4
Kos J F and Bavton R J 1979 *Can. J. Phys.* **57** 1579–88
Kuckhermann V, Thummes G and Mende H H 1985 *J. Phys. F: Met. Phys.* **15** L153–9
Lawrence W E, Wei Chen and Swihart J C 1986 *J. Phys. F: Met. Phys.* **16** L49–54
Nakamura F, Ogasawara K and Takamura 1976 *J. Phys. F: Met. Phys.* **6** L11–5
Neighbor J E and Newbower R S 1969 *Phys. Rev.* **186** 649–50
Nordheim L 1934 *Act. Sci. et Ind.* vol 131 (Paris: Hermann)
Olsen J L 1958 *Helv. Phys. Acta* **31** 713–26
Parrot J E 1965 *Proc. Phys. Soc.* **85** 1143–55
Probst P A, MacInnes M W and Huguenin R 1981 *J. Low Temp. Phys.* **41** 115–65
Rahn J P, Sabo J J and Weir J E 1972 *Phys. Rev.* B **6** 4406–12
Reynolds C L and Anderson A C 1976 *Cryogenics* **16** 687
Ribot J H J, Bass J, van Kempen H and Wyder P 1979 *J. Phys. F: Met. Phys.* **9** L117–22
Risnes R and Sollien V 1969 *Phil. Mag.* **20** 895–905
Risnes R 1970 *Phil. Mag.* **21** 591–7
Romero J, Van der Maas J and Huguenin R 1988 *Helv. Phys. Acta* **61** 149–52
Rowlands J A, Stackhouse B J and Woods S B 1978 *J. Phys. F: Met. Phys.* **8** 2545–58
Rowlands J A and Woods S B 1975 *J. Phys. F: Met. Phys.* **5** L100–3
Sambles J R and Elsom K C 1980 *J. Phys. F: Met. Phys.* **10** 1487–94
—— 1985 *J. Phys. F: Met. Phys.* **15** 161–7
Sambles J R and Mundy J N 1983 *J. Phys. F: Met. Phys.* **13** 2281–92
Sambles J R and Preist T W 1982 *J. Phys. F: Met. Phys.* **12** 1971–87
Soffer S B 1967 *J. Appl. Phys.* **38** 1710–5
Stesmans A 1982 *J. Phys. F: Met. Phys.* **12** 1989–2018
—— 1983 *Phys. Rev.* B **27** 1348–51
Thummes G, Kuckhermann V and Mende H H 1985 *J. Phys. F: Met. Phys.* **15** L65–9
Trattner D, Zehetbauer M and Groger V 1985 *Phys. Rev.* B **31** 1172–3
Tsoi V S, Bass J, Benistant P A M, van Kempen H, Payens E L M and Wyder P 1979 *J. Phys. F: Met. Phys.* **9** L221–6
van Vucht R J M, van de Walle G F A, van Kempen H and Wyder P 1986 *J. Phys. F: Met. Phys.* **16** 1525–36
van der Maas J 1984 *PhD Thesis* Université de Lausanne
van der Maas J, Dalimin M N B and Caplin A D 1981a *Physica B* **107** 141–2
van der Maas J and Huguenin R 1987 *Japan. J. Appl. Phys. Suppl.* 3 **26** 653–4

van der Maas J, Huguenin R and Gasparov V A 1985 *J. Phys. F: Met. Phys.* **15** L271–8
van der Maas J, Huguenin R and Rizzuto C 1981b *Physica* B **107** 139–40
van der Maas J, Rizzuto C and Huguenin R 1981c *Recent Developments in Condensed Matter Physics* vol 2, ed J T Devreese *et al* (New York: Plenum) pp 63–71
—— 1983 *J. Phys. F: Met. Phys.* **13** L53–8
Watts B R 1985 *J. Phys. F: Met. Phys.* **15** 1437–40
Yu Z-Z, Haerle M, Swart J W, Bass J, Pratt W P Jr and Schroeder P A 1984 *Phys. Rev. Lett.* **52** 368–71
Zhao J, Pratt W P, Sato H, Schroeder P A and Bass J 1988 *J. Phys. Rev.* B **37** 8738–48
Ziman J M 1960 *Electrons and Phonons* (Oxford: Oxford University Press) p 451–82